

Journal of Materials Chemistry C

Accepted Manuscript



This article can be cited before page numbers have been issued, to do this please use: P. Rajamalli, V. Thangaraji, S. Natarajan, R. Chen-Cheng, H. Lin and C. H. Cheng, *J. Mater. Chem. C*, 2017, DOI: 10.1039/C7TC00457E.



This is an Accepted Manuscript, which has been through the Royal Society of Chemistry peer review process and has been accepted for publication.

Accepted Manuscripts are published online shortly after acceptance, before technical editing, formatting and proof reading. Using this free service, authors can make their results available to the community, in citable form, before we publish the edited article. We will replace this Accepted Manuscript with the edited and formatted Advance Article as soon as it is available.

You can find more information about Accepted Manuscripts in the [author guidelines](#).

Please note that technical editing may introduce minor changes to the text and/or graphics, which may alter content. The journal's standard [Terms & Conditions](#) and the ethical guidelines, outlined in our [author and reviewer resource centre](#), still apply. In no event shall the Royal Society of Chemistry be held responsible for any errors or omissions in this Accepted Manuscript or any consequences arising from the use of any information it contains.



Journal Name

ARTICLE

Thermally activated delayed fluorescence emitters with a *m,m*-di-*tert*-butyl-carbazolyl benzoylpyridine core achieving extremely high blue electroluminescence efficiencies

Pachaiyappan Rajamalli,^a Vasudevan Thangaraji,^a Natarajan Senthilkumar,^a Chen-Cheng Ren-Wu,^b Hao-Wu Lin^b and Chien-Hong Cheng^{*a}

Received 00th January 20xx,
Accepted 00th January 20xx

DOI: 10.1039/x0xx00000x

www.rsc.org/

Thermally activated delayed fluorescence (TADF) emitters are attractive for the display and lighting applications. Here, a series of highly efficient blue TADF emitters including 3,5-bis((3,6-di-*tert*-butyl-9*H*-carbazol-9-yl)phenyl)(pyridin-4-yl)methanone (4BPY-*m*DTC), (3,5-bis(3,6-di-*tert*-butyl-9*H*-carbazol-9-yl)phenyl)(pyridin-3-yl)methanone (3BPY-*m*DTC), (3,5-bis(3,6-di-*tert*-butyl-9*H*-carbazol-9-yl)phenyl)(pyridin-2-yl)methanone (2BPY-*m*DTC) and (3,5-bis(3,6-di-*tert*-butyl-9*H*-carbazol-9-yl)phenyl)(phenyl)methanone (BP-*m*DTC) were designed and synthesized. The molecular structures feature two meta carbazole substituents attached to a benzoylpyridine (BPY) group or to a benzophenone (BP) group. These compounds show high thermal stability ($T_d = 371 \sim 439 \text{ }^\circ\text{C}$), blue emissions (458 \sim 488 nm), high photoluminescence quantum yields in thin films (PLQY) (75 \sim 96%) and very small energy gaps between S_1 and T_1 (ΔE_{ST}) of 0.01 \sim 0.05 eV. In addition, they all reveal TADF properties including small ΔE_{ST} , two components in the transit PL decays, the prompt emission and the temperature-dependent delayed emission. The BPY series appears to give much higher photoluminescence quantum yields (PLQY >92%) than that of BP-*m*DTC (75%) plausibly due to the more rigid structure caused by the interaction between pyridine nitrogen and the aromatic C-H bond. Further, 4BPY-*m*DTC shows more delayed component compared to 3BPY-*m*DTC and 2BPY-*m*DTC. The electroluminescence devices based on 4BPY-*m*DTC and 2BPY-*m*DTC as the dopant emitters exhibit sky blue emission with maximum external quantum efficiencies (EQEs) over 28%, and current and power efficiency and maximum luminance up to 67.0 cd A⁻¹, 60.1 lm W⁻¹ and 20000 cd m⁻², respectively. The presence of pyridine ring and the position of nitrogen atom in the molecules are critical for the high quantum yield and device efficiency. The PLQY EQE and luminance are dramatically improved by changing the phenyl into the pyridine group in the dopant in these devices.

1. Introduction

Intensive research has continued to focus on OLEDs due to many performance advantages such as access to flexible panels, low power consumption, wider viewing angles, a higher contrast ratio, faster response times, high luminous efficiency, facile color tuning of emitters and are lighter in weight.¹⁻³ Because of the reduced energy consumptions of OLEDs, electronic companies have invested significantly for adopting this forefront technology as a tool to reduce the electricity usage across the world. In the past few decades, intensive research towards OLEDs has successively led to development of different generations of dopant materials such as

fluorescence (1st generation), phosphorescence (2nd generation).⁴⁻¹⁰ The radiative decay of triplet excitons (75%) is spin-forbidden in the fluorescent OLED, and only singlet excitons (25%) can be recruited to produce light.⁴ In the 2nd generation materials of late transition metal complexes as emitters access the emissive triplet states due to singlet-triplet state mixing via efficient spin-orbit coupling, and thus they can harvest both singlet and triplet excitons (100%).¹¹⁻¹⁸ However, the 2nd generation phosphorescent emitters containing precious metals, such as Ir and Pt are expensive and bespoke blue-emitting complexes remains unreliable in terms of their performance in OLED devices for practical applications. Very recently, TADF materials (3rd generation) have been realized for the efficient OLED display and lightings.¹⁹⁻²⁶ Among these three generation materials, TADF materials (3rd generation) have rapidly gained great attentions owing to their high device efficiencies by harvesting 100% of the excitons without requiring the expensive noble metals.

^a Department of Chemistry, National Tsing Hua University, Hsinchu 30013, Taiwan.

^b Department of Materials Science and Engineering, National Tsing Hua University, Hsinchu 30013, Taiwan.

*Email - chcheng@mx.nthu.edu.tw

Electronic Supplementary Information (ESI) available: [General information, computational details, UV-Vis, PL, single crystal packing, CV, TGA, EL spectra, Luminance vs power efficiency]. See DOI: 10.1039/x0xx00000x

ARTICLE

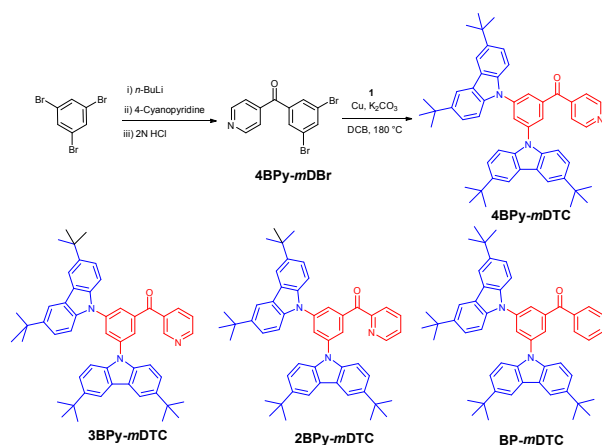
Journal Name

Although many TADF emitters have been developed for red, green, and blue emitting OLEDs.²⁷⁻³² The molecular design for efficient blue TADF emitters is not very clear and systematic plan for the rational molecular designs are highly desired. Particularly, to achieve inexpensive OLEDs for commercial application, there is an urgent need for highly efficient blue emitting materials to overcome the weakness of currently existing blue emitters. In principle, TADF originates from molecules with a small energy gap between the lowest singlet (S_1) and triplet (T_1) excited states that enable the harvesting of both singlet and triplet excitons under electrical excitation.³³⁻⁴⁰ The molecular design plays a critical role in achieving high efficiency of the TADF based OLEDs.²⁹⁻³² Here, we present an ideal simple molecular design for blue TADF emitters consisting of a benzoylpyridine and a benzophenone core as the electron accepting unit and two di(*t*-butyl)carbazole groups as the electron donating units. Importantly, the molecules show very small ΔE_{ST} and extremely high photoluminescence quantum yield (PLQY) in the thin films indicating that they are ideal TADF materials. By using these new TADF materials as emitters, the blue OLEDs can achieve an external quantum efficiency over 28%. These results will open up a new path to achieve efficient blue TADF devices.

2. Results and discussion

2.1. Synthesis and DFT calculation

We have designed and synthesized four TADF materials, including 4BPY-*m*DTC, 3BPY-*m*DTC, 2BPY-*m*DTC, and BP-*m*DTC. The structures of these species consist of a benzoylpyridine and a benzophenone core as the electron accepting unit and two di(*t*-butyl)carbazole groups attached to the *meta* positions of the central phenyl ring as the electron donating units. These four compounds were synthesized in high yields via the Ullmann coupling reaction of 3,6-di-*tert*-butyl-9*H*-carbazole (**1**) with the corresponding *meta* di-bromobenzoyl pyridine derivatives (Scheme 1), while the details of synthetic procedures are given in the Experimental section.



Scheme 1. Synthetic scheme for 4BPY-*m*DTC and structure of 3BPY-*m*DTC, 2BPY-*m*DTC and BP-*m*DTC

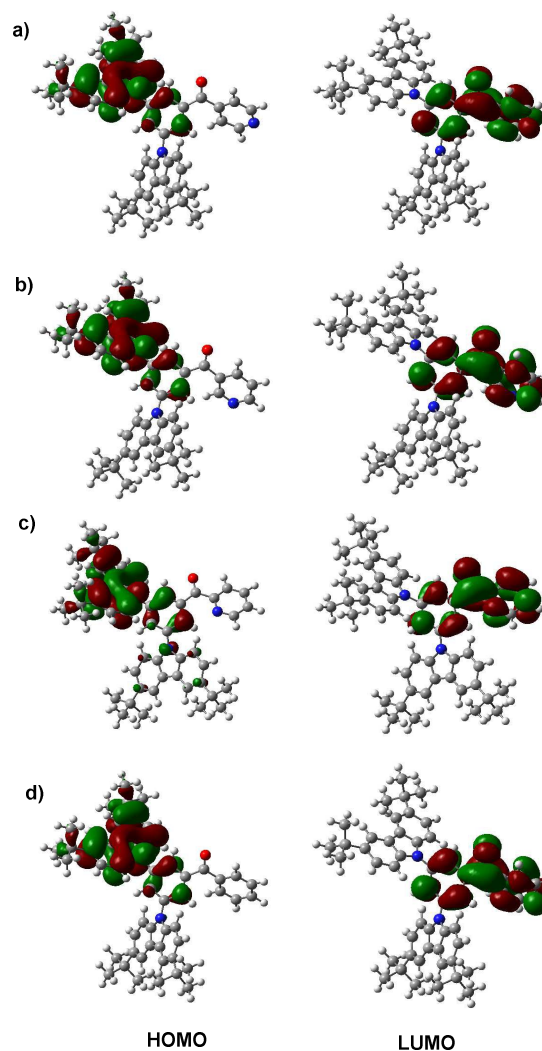


Fig.1 Molecular orbitals of a) 4BPY-*m*DTC, b) 3BPY-*m*DTC, c) 2BPY-*m*DTC and d) BP-*m*DTC.

In these four compounds, the reactive C3 and C6 positions of the carbazole groups were protected by a *t*-butyl group to improve the chemical and electrochemical stability and to enhance the PLQY.²⁹ In addition, the carbonyl acceptor unit is more stable compared to the phosphine oxide or sulfone counterpart.⁴¹ These synthesized emitters were purified by the temperature gradient vacuum sublimation and were characterized by NMR spectroscopy and high-resolution mass spectrometry. The purity of the materials was confirmed by high performance liquid chromatography (HPLC) analysis given in the Experimental section and Supporting Information.

To gain insight into the electronic states of these compounds, time-dependent density functional theory (TD-DFT) calculations were performed for all the compounds at the B3LYP/6-31G (d,p) level. As shown in Fig.1, the LUMOs of 4BPY-*m*DTC, 3BPY-*m*DTC, and 2BPY-*m*DTC are localized on the benzoylpyridine group, and BP-*m*DTC is on the benzophenone moiety due to the strong electron withdrawing

nature of these moieties. Although both *t*-butyl carbazole units are attached *meta* to the pyridoyl or benzoyl unit, the HOMO is mainly on one *t*-butylcarbazole group, and the HOMO-1 are distributed over the other *t*-butylcarbazole. The main transitions of these materials along with oscillator strengths and contour plots of the occupied and unoccupied molecular orbitals are listed in Tables S1-S4. The two carbazolyl groups are slightly different in energy because they interact differently with the pyridoyl unit or benzoyl unit. The separated frontier molecular orbitals lead to small calculated ΔE_{ST} values of 0.13, 0.19, 0.11 and 0.15 eV for 4BPY-*m*DTC, 3BPY-*m*DTC, 2BPY-*m*DTC and BP-*m*DTC, respectively. Besides, in all the molecules, the HOMO and HOMO-1 are extended to the central phenyl linker and show weakly overlap between HOMO and LUMO, which can ensure efficient radiative decay and high PL quantum efficiency.

2.2. Photophysical properties

The UV-vis absorption and PL spectra of these compounds in toluene solutions are depicted in Fig. 2 and Fig. S1 while their physical parameters are summarized in Table 1. The absorption before 350 nm is probably from the $\pi \rightarrow \pi^*$ transitions and weak broadband at 392 nm is assigned to the intramolecular

photoexcitation, the 4BPY-*m*DTC, 3BPY-*m*DTC, 2BPY-*m*DTC and BP-*m*DTC solutions emit sky blue light with PL emission peaks centered at 495, 480, 494 and 465, respectively. All the compounds display significant positive solvatochromic effects of its fluorescent emission in different solvents (Fig. S2). These results suggest that these donor-acceptor molecules show strong charge transfer property from *t*-butylcarbazole to benzoylpyridine or benzophenone and are in good agreement with the DFT calculation (*vide supra*).

From the onset of fluorescence spectra of these compounds, the singlet energies were calculated to be 2.82, 2.90, 2.78 and 2.98 eV for 4BPY-*m*DTC, 3BPY-*m*DTC, 2BPY-*m*DTC, and BP-*m*DTC, respectively (Table 1). The phosphorescent emission spectra of these compounds were measured at 77 K in toluene (10^{-5} M) and are shown in Fig. 1 and Fig. S1. The triplet energies were calculated to be 2.81, 2.85, 2.76 and 2.95 eV for 4BPY-*m*DTC, 3BPY-*m*DTC, 2BPY-*m*DTC, and BP-*m*DTC, respectively, from the onset of phosphorescence spectra. The ΔE_{ST} was estimated to be 0.01 eV for 4BPY-*m*DTC, 0.05 for 3BPY-*m*DTC, 0.02 for 2BPY-*m*DTC and 0.03 eV for BP-*m*DTC, indicating that they plausibly possess TADF property with efficient up-conversion from T_1 to S_1 .²⁹ The ΔE_{ST} calculated are very small (0.01–0.05 eV) for these four molecules in toluene indicating that they plausibly possess TADF property with efficient up-conversion from T_1 to S_1 . In addition, 4BPY-*m*DTC and 2BPY-*m*DTC show very small ΔE_{ST} compared to the 3BPY-*m*DTC and benzophenone unit (BP-*m*DTC).

The electrochemical properties of these materials were investigated by Cyclic Voltammetry (CV) and are shown in Fig. S3. The CV shows reversible oxidation curves for all the compounds, indicating promising electrochemical stability. The HOMO levels were estimated to be -5.65, -5.60, -5.61 and -5.65 eV for 4BPY-*m*DTC, 3BPY-*m*DTC, 2BPY-*m*DTC, and BP-*m*DTC, respectively, obtained from the onset of oxidation waves (*vs* Fc/Fc⁺). The LUMO levels were estimated from HOMO - E_s to be -2.83, -2.71, -2.82, and -2.65 eV for 4BPY-*m*DTC, 3BPY-*m*DTC, 2BPY-*m*DTC, and BP-*m*DTC, respectively. To further study the photophysical property in thin film, the doped films of these materials in a host matrix of 3, 3'-bis(carbazol-9-yl)-1,1'-biphenyl (*m*CBP) were prepared by vacuum deposition at a concentration of 7 wt%. In oxygen-free toluene solutions, the quantum yields are 7.5%, 7.0%, 7.2% and 7.3% for 4BPY-*m*DTC, 3BPY-*m*DTC, 2BPY-*m*DTC and BP-*m*DTC, respectively. In the presence of oxygen, the values decrease to 1.7%, 1.9%, 1.9% and 2.0%. The quantum yield decrease of these compounds in the presence of oxygen supports that these molecules possess TADF property. It is known that the T_1 states of these molecules are readily quenched by the triplet ground state of oxygen molecules leading to the decrease of RISC and subsequently the fluorescence intensity.

Surprisingly, the PLQYs of 7 wt% 4BPY-*m*DTC, 3BPY-*m*DTC, 2BPY-*m*DTC, and BP-*m*DTC doped in *m*CBP thin films are 97, 92, 96 and 75%, respectively, measured using an integrating sphere under N₂ atmosphere. These values are much

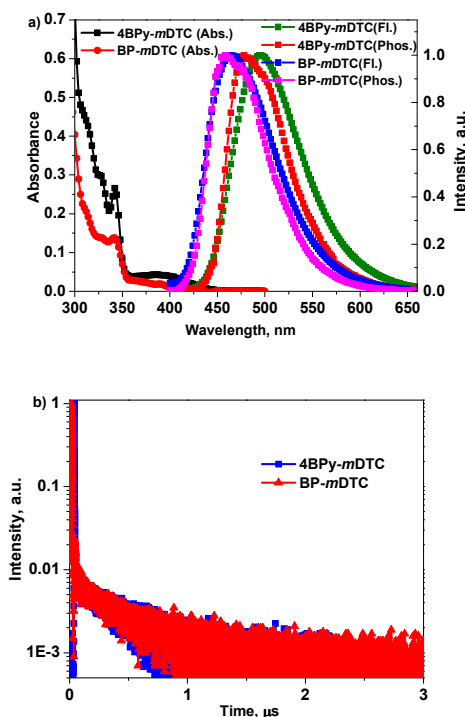


Fig. 2 a) Absorption (Abs.) and fluorescence (Fl.) spectra in toluene (10^{-5} M) measured at room temperature and phosphorescence (Phos.) spectra in toluene (10^{-5} M) measured at 77 K; b) their transient PL characteristics in toluene (10^{-5} M) at room temperature under vacuum.

charge transfer (ICT) absorption associated with the electron transfer from the *t*-butylcarbazole groups to the benzoylpyridine or benzophenone moiety. Upon

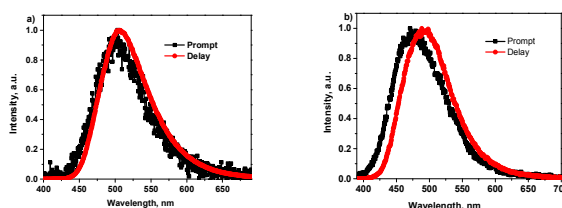
Table 1. Physical properties of 4BPY-*m*DTC, 3BPY-*m*DTC, 2BPY-*m*DTC and BP-*m*DTC

Dopant	λ_{abs} (nm) ^a	λ_{em} (nm) ^a	λ_{em} (nm) ^b	T_d (°C) ^c	HOMO (eV) ^d	LUMO (eV) ^e	E_g (eV) ^f	E_T (eV) ^g	ΔE_{ST} (eV) ^h	Φ_{PL} (%) Sol ⁱ /film(%) ^j	τ_p (ns)/ τ_d (μ s) ⁱ
4BPY- <i>m</i> DTC	342, 396	495	478	408	-5.65	-2.83	2.82	2.81	0.01	7.5/97	28.1/18.0
3BPY- <i>m</i> DTC	339, 381	480	476	439	-5.61	-2.71	2.90	2.85	0.05	7.0/92	4.7/8.3
2BPY- <i>m</i> DTC	342, 394	494	488	411	-5.60	-2.82	2.78	2.76	0.02	7.2/96	5.3/6.9
BP- <i>m</i> DTC	341, 391	465	458	371	-5.63	-2.65	2.98	2.95	0.03	7.3/75	6.1/12.4

^a Measured in toluene (1×10^{-5} M) at room temperature. ^b Phosphorescence measured in toluene (1×10^{-5} M) at 77 K. ^c Obtained from TGA measurements. ^d Measured from the oxidation potential in 10^{-3} M DCM solution by cyclic voltammetry. ^e Calculated from HOMO - LUMO. ^f Estimated from the onset of fluorescence spectrum. ^g Estimated from the onset of phosphorescence spectrum. ^h $\Delta E_{ST} = E_S - E_T$. ⁱ Measured in degassed toluene solution using diphenyl anthracene as a standard. ^j Absolute total PL quantum yield evaluated for 7 wt% dopant in *m*CBP film using an integrating sphere. ^k PL lifetimes of the prompt (τ_p) and delayed (τ_d) decay components in 7 wt%-doped *m*CBP film

higher than those in the solution. This quantum yield enhancement is probably due to the suppression of intramolecular rotational and collisional quenching in the solid state.^{29, 42} The emission spectra of the doped films were shown in Fig. S4. The results reveal that the emissions are only from the dopants. It is noteworthy that the three benzoylpyridine (BPY) derivatives show higher quantum yields compared to the benzophenone (BP) derivative. Further, the BPY derivatives with the nitrogen atom at 4 (4BPY-*m*DTC) and 2 (2BPY-*m*DTC) position of the pyridine ring show slightly higher PLQY (97 and 96%, respectively) compared to that with the nitrogen atom at 3 (3BPY-*m*DTC) position (92% for 3BPY-*m*DTC). The presence of the nitrogen atom and the position in the acceptor unit appear to play an essential role in the fine tuning of the structures to reach very high quantum yield.^{43,44}

To further examine the emission properties of these compounds, prompt and delayed spectra of the co-doped thin films *m*CBP: 4BPY-*m*DTC (7 wt%) and *m*CBP: BP-*m*DTC (7 wt%) were measured (Fig. 3a and 3b). The prompt and delayed spectra coincide with each other for the 4BPY-*m*DTC co-doped film. On the other hand, a slight redshift of the delayed fluorescence relative to the prompt spectrum was observed for BP-*m*DTC. The slight redshift of BP-*m*DTC co-doped film is likely from the conformation change in the thin film: the excited state undergoes conformation adjustment during the RISC to a slightly lower S_1 state.⁴⁵ We suggest that the nitrogen atom restricts the excited state conformational changes via hydrogen bonding in the thin film, which is important in improving the PLQYs in the thin film. The thermal properties of these emitters were determined by thermogravimetric analysis (TGA) under a nitrogen atmosphere and the thermograms are shown in Fig. S5 and the values are summarized in Table 1. The results show that all four compounds possess very high T_d with 4BPY-*m*DTC, 3BPY-*m*DTC, and 2BPY-*m*DTC ~ 40 °C higher than BP-*m*DTC. The high T_d values are important for high morphological stability in the film.

**Fig. 3** Prompt and delayed PL spectra of the co-doped thin films, a) *m*CBP: 4BPY-*m*DTC (7 wt%) and b) *m*CBP: BP-*m*DTC (7 wt%) measured at 300 K.

To confirm the TADF property, the transient PL decay characteristics of these materials were measured in 10^{-5} M toluene solution under vacuum and are shown in Fig. 2b. As shown in Fig. 2b, the transient decay curves can be divided into two components. The first one is the prompt emission decay from S_1 to ground state S_0 with a lifetime (τ) of 2.0 ns and 5.7 ns for 4BPY-*m*DTC and BP-*m*DTC, respectively. The second component is a delayed emission with a lifetime τ of 0.46 μ s and 0.49 μ s for 4BPY-*m*DTC and BP-*m*DTC, respectively. These delayed emissions can be explained as the up-conversion of T_1 to S_1 , followed by fluorescence to the ground state. Further evidence for the TADF property of these materials is from the temperature dependent transient PL decays of co-doped thin films of *m*CBP:4BPY-*m*DTC (7 wt%) and *m*CBP:BP-*m*DTC (7 wt%) measured at 100, 200 and 300 K (Fig. 4a and 4b). The results reveal that the delayed component intensified when the temperature increases. This observation clearly demonstrates that the delayed emission is an RISC process activated by the thermal energy and is a characteristic of TADF emitter.²⁹⁻³² As shown in S6, 4BPY-*m*DTC in the *m*CBP film shows more delayed component than 3BPY-*m*DTC and 2BPY-*m*DTC in their transient PLs at 300 K. The lifetimes of prompt and delayed components of these compounds in the *m*CBP co-doped thin films are summarized in Table 1.

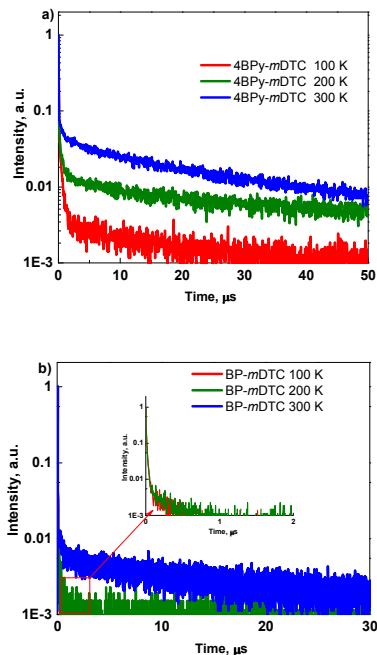


Fig. 4 Temperature dependent transient PL decays of doped films a) *mCBP*: 4BPY-*mDTC* (7 wt%) and b) *mCBP*: BP-*mDTC* (7 wt%) ranging from 100 K to 300 K.

2.3. Electroluminescence performance

To investigate the electroluminescence properties of these TADF materials, multilayer devices A, B, C and D were fabricated using 4BPY-*mDTC*, 3BPY-*mDTC*, 2BPY-*mDTC* and BP-*mDTC* as the dopants, respectively. The molecular structures used in the devices are shown in Fig. S7. Devices A-D were constructed with the following device structure: ITO/NPB (30 nm)/TAPC (20 nm)/*mCBP*:dopant (7 wt%) (30 nm)/DPEPO (5 nm) or PPT (10 nm)/TmPyPb (60 nm)/LiF (0.8 nm)/Al (100 nm). In the devices, *N,N'*-bis(1-naphthyl)-*N,N'*-diphenyl-1,1'-biphenyl-4,4'-diamine (NPB) acts as a hole injection material, 1,1-bis[4-*N,N'*-di(ptyl)amino]phenyl] cyclohexane (TAPC) as a hole-transporting material, 3,3'-bis(*N*-carbazolyl)-1,1'-biphenyl (*mCBP*) as a host material, 1,3,5-tri(*m*-pyrid-3-yl-phenyl)benzene (TmPyPb) is the electron-transporting material. In addition, (oxybis(2,1-phenylene))bis(diphenylphosphine oxide) (DPEPO) or dibenzo[*b,d*]thiophene-2,8-diylbis(diphenylphosphine oxide) (PPT) is used as an exciton blocker for devices A and B-D, respectively. The electroluminescent properties of these devices are displayed in Fig. 5, Fig. S8 and summarized in Table 2.

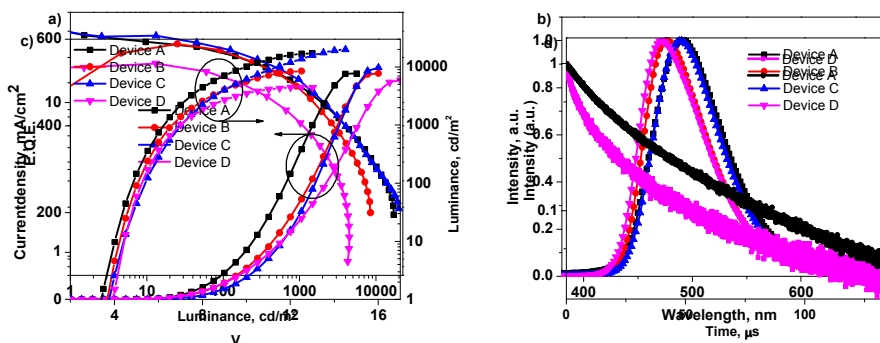


Fig. 5 The EL characteristic plots of devices A-D: a) external quantum efficiency vs luminance, b) electroluminescent spectra, c) current density and luminance vs driving voltage, d) transient electroluminescence characteristics of devices A and D.

Table 2. EL performances of the devices using 4BPy-*m*DTC, 3BPy-*m*DTC, 2BPy-*m*DTC and BP-*m*DTC^{a,b}

Device	dopant	V_d (V) ^b	L (cd m ⁻² , V)	EQE (% , V)	CE (cd A ⁻¹ , V)	PE (lm W ⁻¹ , V)	λ_{max} (nm)	CIE (x,y), 8V
A	4BPy- <i>m</i> DTC	3.3	17038 (13.0)	28.1 (3.5)	67.0 (3.5)	60.1 (3.5)	490	(0.17;0.37)
B	3BPy- <i>m</i> DTC	3.6	8470 (12.5)	24.6 (4.5)	49.1 (4.5)	34.2 (4.5)	476	(0.15;0.28)
C	2BPy- <i>m</i> DTC	3.6	20000 (14.5)	28.0 (4.0)	65.4 (4.5)	50.7 (4.0)	490	(0.16;0.37)
D	BP- <i>m</i> DTC	3.8	4475 (12.5)	18.2 (4.5)	34.6 (4.5)	25.4 (4.0)	472	(0.15;0.25)
E	Flrpic	3.3	27332 (12.0)	18.7 (3.5)	34.6 (3.5)	30.9 (3.5)	462	(0.15;0.25)

^aDevice configuration for A-D: ITO/NPB (30 nm)/TAPC (20 nm)/*m*CBP: dopant (7 wt%) (30 nm)/DPEPO (5 nm) (Device A) or PPT (10 nm) (Devices B-D)/TmPyPb (60 nm)/LiF (0.8 nm)/Al (100 nm), respectively; ^b V_d , The operating voltage at a brightness of 1 cd m⁻²; L, maximum luminance; EQE, maximum external quantum efficiency; CE, maximum current efficiency; PE, maximum power efficiency; and λ_{max} , the wavelength where the EL spectrum has the highest intensity.

The EQE vs luminance of devices A-D is shown in Fig. 5a. Devices A and C gave sky blue electroluminescence with EQEs of 28.1 and 28.0%, respectively. These efficiencies are much higher than the earlier reported device based on a carbazole derived blue TADF emitter (EQE~18%).²⁷ The current and power efficiency of devices A and C are 67.0 and 65.4 cd A⁻¹ and 60.1 and 50.7 lm W⁻¹, respectively. Moreover, device C with 2BPy-*m*DTC as the dopant emitter showed a maximum luminance of 20000 cd m⁻² without any light out-coupling enhancement. On the other hand, the maximum EQE and luminance of devices B and D drop to 24.6 and 18.3% and 8470 cd m⁻² and 4475 cd m⁻², respectively. Although BP-*m*DTC shows lower ΔE_{ST} of 0.03 eV than that of 3BPy-*m*DTC (0.05 eV), the EQE of 3BPy-*m*DTC-based device B is much higher than that of BP-*m*DTC-based device D. This observation may be explained by the substantially higher PLQY of 3BPy-*m*DTC in the *m*CBP thin film and the presence of the pyridine group likely accounts for the higher PLQY. Surprisingly, 4-pyridine (4BPy-*m*DTC) and 2-pyridine (2BPy-*m*DTC) derived compounds show higher luminance (17000–20000 cd m⁻²) than the 3-pyridine (3BPy-*m*DTC) derivative (8470 cd m⁻²). Also, the 4-pyridine derivative shows low turn-on voltage (3.3 V) compared 2-pyridine and 3-pyridine (3.6 V) derivatives, due to the enhanced electron transporting ability of 4-pyridine.⁴⁶ These results suggest that the position of the nitrogen atom in the molecules is vital to the luminance and the operating voltage.

The EL performance of these devices is in the order A \approx C > B \gg D. The EQE and luminance were dramatically improved by changing the phenyl to a pyridine group in the dopant in these devices. This can be attributed to the substantially lower PLQY of BP-*m*DTC relative to the corresponding values of the BPy series. Further, the lower device efficiency of 3BPy-*m*DTC-based device B relative to 4BPy-*m*DTC-based A and 2BPy-*m*DTC-based C is also likely due to the slightly lower PLQY of 3BPy-*m*DTC and the slightly higher ΔE_{ST} compared to those of the other two materials.

The electroluminescence (EL) spectra are presented in Fig. 5. They are similar to the corresponding PL spectra of the four

emitters, confirming that the EL emissions are from the fluorescence of the emitters. The EL peak positions of devices A, B, C and D appear at 490, 476, 490 and 472 nm, respectively without emission from other materials. The color coordinates of the devices are listed in Table 2 along with device performances. To check the device emission stability at various operating voltages, the EL spectra were measured from 6 to 12 V and no significant change of the spectra with applied voltage was observed for all the devices (Fig. S9). To compare the device performance with the standard blue phosphorescent emitter (Flrpic), device E was fabricated with the device structure similar to B-D except that Flrpic is used as the dopant and the device performance is shown in Fig. S10 and summarized in Table 2. The observed EQE for device E is ~18.7% and is comparable to the reported Flrpic based device.⁴⁶ As shown in Table 2 and Fig. 5, devices A, B and C with 4BPy-*m*DTC, 3BPy-*m*DTC and 2BPy-*m*DTC as the dopants, respectively, surpass device E in terms of EQE, current efficiency, and power efficiency. These results reveal that TADF emitters have the potential as the replacement for the expensive blue phosphorescent emitters.

Furthermore, to confirm the TADF property of the devices, the transient electroluminescence decays for devices A-D were measured at room temperature under electrical excitation. Fig. 5d and Fig. S11 show that the delayed electroluminescence component lasts for several tens of microseconds with a very high delayed component. The results indicate that the EL efficiency is largely contributed by the delayed fluorescence, supporting the importance of TADF process in these devices. Device A shows a stronger delayed component compared to device D; this observation is consistent with the observed device performance. The RISC process is more efficient under electrical excitation for device A (4BPy-*m*DTC) than for device D (BP-*m*DTC) (Fig. 5d).

3. Experimental section

3.1. Synthesis of the target molecules

3.1.1. Synthesis of (3,5-bis(3,6-di-*tert*-butyl-9*H*-carbazol-9-yl)phenyl)(pyridin-4-yl)methanone (4BPY-*m*DTC). To an oven dried seal tube (3,5-dibromophenyl)(pyridine-4-yl)methanone (4BPY-*m*DBr) (2.50 g, 7.33 mmol), *t*-butyl carbazole (5.11 g, 18.3 mmol), Cu (0.93 g, 14.7 mmol), K₂CO₃ (5.06 g, 36.7 mmol) and 1,2-dichlorobenzene (20 mL) was added. The system was evacuated and was purged with nitrogen and the mixture was heated with stirring at 180 °C for 48 h. After completion of the reaction, the reaction mixture was filtered through Celite and washed with ethyl acetate (50 mL). The combined filtrate was evaporated under reduced pressure and the residue was purified by column chromatography using 25% ethyl acetate/*n*-hexane as eluent to afford 4BPY-*m*DTC in 78% yield. ¹H NMR (400 MHz, CDCl₃): δ 8.84 (d, *J* = 5.2 Hz, 2 H), 8.13 (s, 4 H), 8.09 (d, *J* = 1.6 Hz, 1 H), 8.04 (d, *J* = 2.0 Hz, 2 H), 7.71 (d, *J* = 5.6 Hz, 2 H), 7.49-7.44 (m, 8 H), 1.44 (s, 36 H); ¹³C NMR (100 MHz, CDCl₃): δ 193.78 (-CO-), 150.67, 143.87, 143.47, 140.42, 139.09, 138.49, 128.54, 125.53, 124.01, 123.87, 122.74, 116.59, 108.84, 34.78, 31.94; HRMS (FAB⁺) cal for C₅₂H₅₅N₃O 737.4345, found 737.4335. **HPLC** (CHIRALCEL OD-H, 4.6 x 250 nm; 10 % *i*-PrOH / hexane, 1.0 mL/min, 254 nm; t_r(100%) = 4.85 min (Fig. S12a).

3.1.2. Synthesis of (3,5-bis(3,6-di-*tert*-butyl-9*H*-carbazol-9-yl)phenyl)(pyridin-3-yl)methanone (3BPY-*m*DTC). A procedure similar to that of 4BPY-*m*DTC was followed for the synthesis of 3BPY-*m*DTC using 3BPY-*m*DBr (2.5 g, 7.33 mmol), *t*-butyl carbazole (5.11 g, 18.33 mmol), Cu (0.93 g, 14.66 mmol), K₂CO₃ (5.06 g, 36.65 mmol) and 1,2-dichlorobenzene (20 mL) in 75% yield. ¹H NMR (400 MHz, CDCl₃): δ 9.17 (s, 1 H), 8.85 (d, *J* = 3.6 Hz, 1 H), 8.24 (d, *J* = 6.0 Hz, 1 H), 8.13 (s, 4 H), 8.09 (t, *J* = 2.0 Hz, 1 H), 8.04 (t, *J* = 2.0 Hz, 2 H), 7.46-7.51 (m, 9 H), 1.45 (s, 36 H); ¹³C NMR (100 MHz, CDCl₃): δ 193.75 (-CO-), 153.75, 151.16, 144.12, 140.68, 140.28, 138.87, 137.45, 132.81, 128.55, 125.79, 124.35, 124.17, 123.90, 116.87, 109.23, 35.08, 32.07; HRMS [ESI, m/z] [M+H]⁺ cal for C₅₂H₅₆N₃O+H⁺: 738.4423, found 738.4423. **HPLC** (CHIRALCEL OD-H, 4.6 x 250 nm; 10 % *i*-PrOH / hexane, 1.0 mL/min, 254 nm; t_r(100%) = 4.04 min (Fig. S12b).

3.1.3. Synthesis of (3,5-bis(3,6-di-*tert*-butyl-9*H*-carbazol-9-yl)phenyl)(pyridin-2-yl)methanone (2BPY-*m*DTC). A procedure similar to that of 4BPY-*m*DTC was followed for the synthesis of 2BPY-*m*DTC using 2BPY-*m*DBr (2.5 g, 7.33 mmol), *t*-butyl carbazole (5.11 g, 18.33 mmol), Cu (0.93 g, 14.66 mmol), K₂CO₃ (5.06 g, 36.65 mmol) and 1,2-dichlorobenzene (20 mL) in 80% yield. ¹H NMR (400 MHz, CDCl₃): δ 8.78 (d, *J* = 4.0 Hz, 1 H), 8.36 (s, 2 H), 8.13-8.19 (m, 5 H), 8.04 (s, 1 H), 7.91-7.95 (t, *J* = 6.4 Hz, 1 H), 7.47-7.57 (m, 9 H), 1.46 (s, 36 H); ¹³C NMR (100 MHz, CDCl₃): δ 192.19 (-CO-), 154.14, 148.72, 143.48, 139.50, 139.23, 138.68, 137.34, 127.58, 127.03, 126.83, 124.80, 123.86, 123.72, 116.40, 109.22, 34.75, 31.97; HRMS (FAB⁺) cal for C₅₂H₅₅N₃O 737.4345, found 737.4349. **HPLC** (CHIRALCEL OD-H, 4.6 x

250 nm; 10 % *i*-PrOH / hexane, 1.0 mL/min, 254 nm; t_r(100%) = 3.58 min (Fig. S12c).

3.1.4. Synthesis of (3,5-bis(3,6-di-*tert*-butyl-9*H*-carbazol-9-yl)phenyl)(phenyl)methanone (BP-*m*DTC). A procedure similar to that of 4BPY-*m*DTC was followed for the synthesis of BP-*m*DTC using (3,5-dibromophenyl)(phenyl)methanone (BP-*m*DBr) (2.5 g, 7.33 mmol), *t*-butyl carbazole (5.11 g, 18.33 mmol), Cu (0.93 g, 14.66 mmol), K₂CO₃ (5.06 g, 36.65 mmol) and 1,2-dichlorobenzene (20 mL) in 71% yield. ¹H NMR (400 MHz, CDCl₃): δ 8.13 (s, 4 H), 8.04 (s, 2 H), 7.93-7.95 (d, *J* = 8.0 Hz, 2 H), 7.60 (t, *J* = 7.2 Hz, 1 H), 7.49-7.53 (m, 11 H), 1.49 (s, 36 H); ¹³C NMR (100 MHz, CDCl₃): δ 195.18 (-CO-), 143.63, 140.90, 139.89, 138.58, 136.73, 133.17, 130.10, 128.63, 127.49, 125.63, 123.92, 123.75, 116.49, 108.99, 34.76, 31.95; HRMS (FAB⁺) cal for C₅₂H₅₅N₂O 736.4393, found 736.4398. **HPLC** (CHIRALCEL OD-H, 4.6 x 250 nm; 10 % *i*-PrOH / hexane, 1.0 mL/min, 254 nm; t_r(100%) = 3.25 min (Fig. S12d).

4. Conclusions

In summary, we have designed and synthesized a series of the TADF emitters, bearing a benzoylpyridine or benzophenone core as the electron-accepting unit and two *meta* *t*-butylcarbazolyl groups as the electron-donating units. These molecules show small Δ*E*_{ST} and very high quantum yields (~97%) in the thin films. The EQE and luminance were dramatically improved from 18 to 28% and from 4475 to 20000 cd m⁻², respectively, by changing a phenyl to a pyridine group in the acceptor units. Among the pyridine derived emitters, 4BPY-*m*DTC and 2BPY-*m*DTC show high efficiency compared to the 3BPY-*m*DTC. The nitrogen atom in the acceptor unit is playing a more vital role than the low Δ*E*_{ST} values for improving the PLQY and EL performances. This work presents a judicious design strategy for tuning TADF materials to achieve excellent sky-blue OLEDs. The light blue emission and the high EL efficiency would make these materials excellent candidates for the practical application in two-color white OLEDs.

Acknowledgements

We thank the Ministry of Science and Technology of Republic of China (MOST 104-2633-M-007-001) for support of this research and the National Center for High-Performance Computing (Account number: u32chc04) of Taiwan for providing the computing time.

Notes and references

- 1 Highly Efficient OLEDs with Phosphorescent Materials (Ed.: H. Yersin), Wiley-VCH, Weinheim, 2008.
- 2 Organic Light-Emitting Devices: Synthesis Properties and Applications (Eds.: K. Müllen; U. Scherf), Wiley-VCH, Weinheim, 2006.
- 3 G. M. Farinola and R. Ragni, *Chem. Soc. Rev.* 2011, **40**, 3467
- 4 H.-H. Chou, Y.-H. Chen, H.-P. Hsu, W.-H. Chang, Y.-H. Chen and C.-H. Cheng, *Adv. Mater.* 2012, **24**, 5867.

ARTICLE

Journal Name

- 5 C. W. Lee and J. Y. Lee, *Adv. Mater.* 2013, **25**, 5450.
- 6 M. C. Gather, A. Köhnen and K. Meerholz, *Adv. Mater.* 2011, **23**, 233.
- 7 K. T. Kamtekar, A. P. Monkman and M. R. Bryce, *Adv. Mater.* 2010, **22**, 572.
- 8 N. Sun, Q. Wang, Y. Zhao, Y. Chen, D. Yang, F. Zhao, J. Chen and D. Ma, *Adv. Mater.* 2014, **26**, 1617.
- 9 G. Schwartz, M. Pfeiffer, S. Reineke, K. Walzer and K. Leo, *Adv. Mater.* 2007, **19**, 3672.
- 10 D. Zhang, M. Cai, Y. Zhang, D. Zhang and L. Duan, *ACS Appl. Mater. Interfaces* 2015, **7**, 28693.
- 11 C. Fan, L. Zhu, T. Liu, B. Jiang, D. Ma, J. Qin and C. Yang, *Angew. Chem. Int. Ed.* 2014, **53**, 2147.
- 12 B.-S. Du, J.-L. Liao, M.-H. Huang, C.-H. Lin, H.-W. Lin, Y. Chi, H.-A. Pan, G.-L. Fan, K.-T. Wong, G.-H. Lee and P.-T. Chou, *Adv. Funct. Mater.* 2012, **22**, 3491.
- 13 K.-Y. Lu, H.-H. Chou, C.-H. Hsieh, Y.-H. O. Yang, H.-R. Tsai, H.-Y. Tsai, L.-C. Hsu, C.-Y. Chen, I. C. Chen and C.-H. Cheng, *Adv. Mater.* 2011, **23**, 4933.
- 14 S. Reineke, T. C. Rosenow, B. Lüssem and K. Leo, *Adv. Mater.* 2010, **22**, 3189.
- 15 S. Reineke, F. Lindner, G. Schwartz, N. Seidler, K. Walzer, B. Lüssem and K. Leo, *Nature* 2009, **459**, 234.
- 16 G. Schwartz, S. Reineke, T. C. Rosenow, K. Walzer and K. Leo, *Adv. Funct. Mater.* 2009, **19**, 1319.
- 17 K. C. Wu, P. J. Ku, C. S. Lin, H. T. Shih, F. I. Wu, M. J. Huang, J. J. Lin, I. C. Chen and C.-H. Cheng, *Adv. Funct. Mater.* 2008, **18**, 67.
- 18 S. R. Forrest, M. A. Baldo and M. E. Thompson, *Nature*, 2000, **403**, 750.
- 19 M. Kim, S. K. Jeon, S.-H. Hwang and J. Y. Lee, *Adv. Mater.*, 2015, **27**, 2515.
- 20 L.-S. Cui, Y.-M. Xie, Y.-K. Wang, C. Zhong, Y.-L. Deng, X.-Y. Liu, Z.-Q. Jiang and L.-S. Liao, *Adv. Mater.*, 2015, **27**, 4213.
- 21 Y. Tao, K. Yuan, T. Chen, P. Xu, H. Li, R. Chen, C. Zheng, L. Zhang and W. Huang, *Adv. Mater.*, 2014, **26**, 7931.
- 22 J. W. Sun, J.-H. Lee, C.-K. Moon, K.-H. Kim, H. Shin and J.-J. Kim, *Adv. Mater.*, 2014, **26**, 5684.
- 23 T. Komino, H. Nomura, T. Koyanagi and C. Adachi, *Chem. Mater.*, 2013, **25**, 3038.
- 24 J. Li, T. Nakagawa, J. MacDonald, Q. Zhang, H. Nomura, H. Miyazaki and C. Adachi, *Adv. Mater.*, 2013, **25**, 3319.
- 25 J. S. Ward, R. S. Nobuyasu, A. S. Batsanov, P. Data, A. P. Monkman, F. B. Dias and M. R. Bryce, *Chem. Commun.*, 2016, **52**, 2612.
- 26 Q. Zhang, T. Komino, S. Huang, S. Matsunami, K. Goushi and C. Adachi, *Adv. Funct. Mater.*, 2012, **22**, 2327.
- 27 P. Rajamalli, N. Senthilkumar, P. Gandeepan, C.-Z. Ren-Wu, H.-W. Lin and C.-H. Cheng, *J. Mater. Chem. C*, 2016, **4**, 900.
- 28 K. Kawasumi, T. Wu, T. Zhu, H. S. Chae, T. Van Voorhis, M. A. Baldo and T. M. Swager, *J. Am. Chem. Soc.*, 2015, **137**, 11908.
- 29 P. Rajamalli, N. Senthilkumar, P. Gandeepan, P.-Y. Huang, M.-J. Huang, C.-Z. Ren-Wu, C.-Y. Yang, M.-J. Chiu, L.-K. Chu, H.-W. Lin and C.-H. Cheng, *J. Am. Chem. Soc.*, 2016, **138**, 628.
- 30 G. Méhes, H. Nomura, Q. Zhang, T. Nakagawa and C. Adachi, *Angew. Chem. Int. Ed.*, 2012, **51**, 11311.
- 31 Q. Zhang, J. Li, K. Shizu, S. Huang, S. Hirata, H. Miyazaki and C. Adachi, *J. Am. Chem. Soc.*, 2012, **134**, 14706.
- 32 M. Y. Wong, G. J. Hedley, G. Xie, L. S. Kölln, I. D. W. Samuel, A. Pertegás, H. J. Bolink and E. Zysman-Colman, *Chem. Mater.*, 2015, **27**, 6535.
- 33 K. Nasu, T. Nakagawa, H. Nomura, C.-J. Lin, C.-H. Cheng, M.-R. Tseng, T. Yasuda and C. Adachi, *Chem. Commun.*, 2013, **49**, 10385.
- 34 Q. Zhang, H. Kuwabara, W. J. Potscavage, S. Huang, Y. Hatae, T. Shibata and C. Adachi, *J. Am. Chem. Soc.*, 2014, **136**, 18070.
- 35 Q. Zhang, D. Tsang, H. Kuwabara, Y. Hatae, B. Li, T. Takahashi, S. Y. Lee, T. Yasuda and C. Adachi, *Adv. Mater.*, 2015, **27**, 2096.
- 36 H. Uoyama, K. Goushi, K. Shizu, H. Nomura and C. Adachi, *Nature*, 2012, **492**, 234.
- 37 Q. Zhang, B. Li, S. Huang, H. Nomura, H. Tanaka and C. Adachi, *Nature Photon.*, 2014, **8**, 326.
- 38 D. R. Lee, M. Kim, S. K. Jeon, S.-H. Hwang, C. W. Lee and J. Y. Lee, *Adv. Mater.*, 2015, **27**, 5861.
- 39 Y. J. Cho, S. K. Jeon, B. D. Chin, E. Yu and J. Y. Lee, *Angew. Chem. Int. Ed.*, 2015, **54**, 5201.
- 40 Y. J. Cho, S. K. Jeon, S.-S. Lee, E. Yu and J. Y. Lee, *Chem. Mater.*, 2016, **28**, 5400.
- 41 N. Lin, J. Qiao, L. Duan, L. Wang and Y. Qiu, *J. Phys. Chem. C* 2014, **118**, 7569.
- 42 S. Gan, W. Luo, B. He, L. Chen, H. Nie, R. Hu, A. Qin, Z. Zhao and B. Z. Tang, *J. Mater. Chem. C*, 2016, **4**, 3705.
- 43 Q. Zhang, T. Komino, S. Huang, S. Matsunami, K. Goushi and C. Adachi, *Adv. Funct. Mater.*, 2012, **22**, 2327.
- 44 F. B. Dias, K. N. Bourdakos, V. Jankus, K. C. Moss, K. T. Kamtekar, V. Bhalla, J. Santos, M. R. Bryce and A. P. Monkman, *Adv. Mater.*, 2013, **25**, 3707.
- 45 K. Goushi, K. Yoshida, K. Sato and C. Adachi, *Nature Photon.*, 2012, **6**, 253.
- 46 C.-H. Shih, P. Rajamalli, C.-A. Wu, W.-T. Hsieh and C.-H. Cheng, *ACS Appl. Mater. Interfaces*, 2015, **7**, 10466.
- 47 H.-H. Chou and C.-H. Cheng, *Adv. Mater.*, 2010, **22**, 2468.

Thermally activated delayed fluorescence emitters with a *m,m*-di-*tert*-butyl-carbazolyl benzoylpyridine core achieving extremely high blue electroluminescence efficiencies

Pachaiyappan Rajamalli,^a Vasudevan Thangaraji,^a Natarajan Senthilkumar,^a Chen-Cheng Ren-Wu,^b Hao-Wu Lin^b and Chien-Hong Cheng^{*,a}

^aDepartment of Chemistry, National Tsing Hua University, Hsinchu 30013, Taiwan.
E-mail: chcheng@mx.nthu.edu.tw

^bDepartment of Materials Science and Engineering, National Tsing Hua University, Hsinchu 30013, Taiwan

High performance blue OLEDs with maximum EQEs over 28% are achieved from TADF emitters bearing a *m,m*-di-*tert*-butyl-carbazolyl benzoylpyridine unit. The heteroatom and position of heteroatom in the molecules are essential for the very high PL quantum yield and device efficiency.

